land

*Article*

# Evaluation of the Impact of Courtyard Layout on Wind Effects on Coastal Traditional Settlements

**Zefa Wang [1,2,3], Tiantian Huang [1], Yaolong Wang [1,*], Shan Dai [4,*], Yuee Zeng [2], Jing Chen [5,6] and Fengliang Tang [1]**

1 School of Architecture, Tianjin University, Tianjin 300072, China
2 School of Resources and Environmental Sciences, Quanzhou Normal University, Quanzhou 362000, China
3 Key Laboratory of Rural Environmental Remediation and Waste Recycling (Quanzhou Normal University), Fujian Province University, Quanzhou 362000, China
4 School of Fine Arts and Design, Quanzhou Normal University, Quanzhou 362000, China
5 Institute of Geography, Fujian Normal University, Fuzhou 350007, China
6 School of Geographical Sciences, Fujian Normal University, Fuzhou 350007, China
* Correspondence: wangyaolong@tju.edu.cn (Y.W.); d_02053@stumail.qztc.edu.cn (S.D.)

**Abstract:** In the context of global climate change, the rising frequency of extreme weather events has increasingly highlighted their impact on human settlements. This study examines the influence of courtyard layout on the wind environment in coastal, traditional villages, focusing on its relevance and importance for enhancing living comfort and preserving cultural heritage. Utilizing data from 204 typical courtyards in Quanzhou City, Fujian Province, China, 18 representative courtyard models were abstracted and analyzed for their winter wind conditions using Computational Fluid Dynamics (CFD) simulations. The study findings indicate (1) that an increase in the courtyard area index gradually decreases wind comfort, with the most optimal wind comfort, stability, and adaptability observed in courtyards of 15 $m^2$, 15 $m^2$, and 110 $m^2$. (2) Wind comfort follows a fluctuating pattern as the aspect ratio changes. Courtyards with aspect ratios of 0.8, 1, and 1.2 demonstrate the highest levels of wind comfort, stability, and adjustability. (3) Wind comfort varies in a wave-like manner depending on orientation, with courtyards facing northeast, southeast, and northwest providing superior wind comfort, stability, and adjustability. These findings offer insights into optimizing courtyard designs to enhance environmental quality and promote sustainable living in coastal, traditional villages.

**Keywords:** wind environment; CFD simulation; on-site testing; courtyard layout; coastal traditional villages



**Citation:** Wang, Z.; Huang, T.; Wang, Y.; Dai, S.; Zeng, Y.; Chen, J.; Tang, F. Evaluation of the Impact of Courtyard Layout on Wind Effects on Coastal Traditional Settlements. *Land* **2024**, *13*, 1813. https://doi.org/10.3390/land13111813

Academic Editor: Zhonghua Gou

Received: 13 September 2024
Revised: 25 October 2024
Accepted: 29 October 2024
Published: 1 November 2024



## 1. Introduction

Global climate change has led to a significant increase in extreme weather phenomena, including floods, droughts, heatwaves, and hurricanes. These events have had a profound impact on human habitats, agriculture, and natural ecosystems. In coastal areas, rising sea levels and intensified wind events significantly impact the design and sustainability of traditional village compounds. Globalization and modernization have further complicated this situation, contributing to rapid urbanization and lifestyle shifts that challenge the preservation of traditional architectural forms. As modern infrastructure and global architectural trends permeate rural areas, local design elements are at risk of being lost, potentially undermining both environmental resilience and cultural heritage.

In this context, the courtyards of traditional villages are more than just spaces for daily activities; they are essential for regulating the microclimate and enhancing living comfort. However, balancing these traditional architectural practices with the pressures of climate adaptation and socio-economic modernization is a growing challenge. Traditional designs need to be reconsidered and improved to cope with both modern needs and environmental challenges. Specifically, in coastal, traditional villages, the distinct geographical and climatic conditions have shaped unique spatial layouts that are crucial for mitigating the impacts of strong sea winds. Thus, it is essential to integrate both ecological wisdom and modern environmental strategies into courtyard designs to enhance the adaptability of these spaces.

Optimizing courtyard design is not only crucial for improving the quality of life of the inhabitants, but also for preserving regional cultural heritage in the face of globalization and modernization. Coastal, traditional villages, characterized by their proximity to the sea and exposure to marine climates, have evolved unique spatial organizations in their village layouts and courtyard configurations to withstand sea winds. Effective courtyard design can enhance residents' comfort and contribute to cultural preservation. However, under the dual pressures of environmental change and modern development, many traditional villages struggle to maintain their distinctive architectural styles. The key research question is how to preserve these traditional features while adapting to contemporary environmental and social demands. This issue transcends technical solutions, requiring a holistic approach that integrates cultural, environmental, and architectural considerations.

Computational Fluid Dynamics (CFD) is a simulation technology that combines numerical calculations and image processing to address engineering challenges. It is widely used to assess the physical environments of various indoor and outdoor spaces, including villages, neighborhoods, buildings, and courtyards. For instance, in Shirakawa Village, Japan, scholars Hayakawa Kishu and Miyaoka Dai utilized CFD to study the effects of local wind directions on terrain, topography, and building layouts [1]. Similarly, Ai Z.T. and Mak C.M. demonstrated that a T-shaped computational domain in CFD simulations effectively predicts the flow fields in urban street canyons, impacting air quality, thermal environments, and risk assessments [2]. In Colombia, Villagrán et al. used CFD to examine how elevating drain heights above multi-tunnel greenhouses affects airflow and thermal distribution, thereby guiding greenhouse design improvements [3]. Emmanuel et al. employed computer simulations to devise strategies to mitigate urban heat islands and enhance urban wind environments through thoughtful building layout and morphology [4]. In North China, Yifei Zhao and colleagues applied the ENVI-met model to investigate how trees influence microclimates and reduce urban heat islands in enclosed courtyards, supporting effective tree placement in urban planning [5]. Furthermore, Chang C. utilized FLUENT 6.3 software to explore the wind environment in streets enclosed by parallel buildings, identifying the relationship between street width-to-height ratios and wind conditions and proposing new design approaches for residential areas [6]. Lastly, using Dimen Dong Village in Guizhou as a case study, Li Zhengrong and his team examined the impacts of building layout, terrain, and topography on the wind environment during different seasons [7].

These examples demonstrate the practicality of CFD simulations for analyzing airflow, temperature, and pressure in diverse settings. Building on this foundation, the current study integrates CFD simulations with field measurements to delve into the wind environment of courtyard spaces in traditional villages, aiming to enhance both comfort and environmental quality.

Research on courtyard spatial layout, primarily focused on traditional villages, streets, and gardens, is still somewhat limited. These studies often employ a combination of field measurements and computer numerical simulations to assess factors such as solar radiation, ventilation, temperature, and humidity within various courtyard layouts. For example, Xiao Yu Ying and Han Xin Yu utilized CFD simulations to explore how the size and wind adaptability of courtyards influence well-known architectural courtyards both domestically and internationally [8]. Dang Yaqi explored the relationship between the courtyard architectural plane enclosure forms and building morphology parameters, examining their impact on improving wind conditions in courtyards [9]. Chen Kexin investigated the effects of different courtyard form combinations on the wind environment in urban residential courtyards in Inner Mongolia, using both field measurements and computer simulations [10]. Lili Zhang et al. studied how courtyard layout and building orientation affect winter winds in Liyuanba Village, Bazhong, Sichuan [11]. Li Yang et al. applied CFD data simulation to compare the wind environments in row and singular courtyard types, finding that row courtyards promote better airflow [12]. İ Sözen et al. analyzed courtyard wind environments with varying influencing factors through CFD simulations, offering recommendations for enhancing environmental quality [13]. Sharples S employed wind tunnel experiments alongside numerical simulations to evaluate six different courtyard building forms, providing optimization strategies for improving wind conditions in various courtyard configurations [14]. Wang Jiao used Fluent software to simulate the wind environment in courtyards, considering variables such as courtyard scale, wall height, enclosure degree, and courtyard form to identify the optimal ventilation indices for each factor [15]. Wang Yansong et al. discussed the impact of open and semi-enclosed spaces on wind comfort during winter and summer using CFD data simulations [16].

Existing research underscores the utility of Computational Fluid Dynamics (CFD) 2016 software in simulating and analyzing the impact of courtyard spatial layouts on the wind environment. This method has gained wide acceptance and application within the academic community. However, the majority of these studies focus on renowned architectural courtyards or traditional dwellings in specific regions, both domestically and internationally. This leaves a significant research gap concerning the wind environments of traditional village courtyards in the coastal areas of southern Fujian. Additionally, most existing studies concentrate on the layout of a single courtyard form and lack a systematic examination of the comprehensive impact of a courtyard spatial form index system—including factors such as courtyard scale, wall height, enclosure degree, and courtyard form—on the wind environment.

To address this gap, future research should aim to evaluate the impact of the courtyard layout index system on the wind environment in traditional village courtyards in these coastal areas. This study specifically focuses on traditional village courtyards, examining how different courtyard layouts affect the outdoor wind environment. Preliminary experiments have identified that comfort in winter courtyard spaces is crucial for outdoor activities in traditional villages. Consequently, this research employs a combination of CFD simulations and field measurements during the winter season to explore the effects of courtyard layout factors on the wind environment. The goal is to validate the ecological design principles that have historically shaped the spatial layout of traditional village courtyards in ancient China.

## 2. Data and Method

### *2.1. Research Subjects: Traditional Village Courtyard Layouts*

#### 2.1.1. Overview of Traditional Village Courtyard Spaces in Quanzhou City, Fujian Province

Quanzhou City, situated on the southeastern coast of China between longitudes 117°25′ to 119°04′ E and latitudes 24°30′ to 25°56′ N, is located in the subtropical marine monsoon zone. This region is characterized by relatively high average annual wind speeds, which present significant challenges to the human wind environment. Quanzhou, often referred to as the hometown of overseas Chinese, is celebrated as the starting point of the ancient "Maritime Silk Road" and has been historically acclaimed as the "largest port in the East" (Figure 1a). As of the end of March 2024, the city boasts 111 traditional villages (at both national and provincial levels). The traditional rural courtyards in Quanzhou are characterized by their enclosed or semi-enclosed layouts, which provide protection from coastal winds while facilitating air circulation within the courtyards. These courtyards commonly incorporate Minnan architectural styles, featuring low-rise buildings arranged around a central courtyard space. Walls and enclosures serve to buffer the wind, while orientations facing southeast or southwest are common to mitigate the effects of dominant wind directions. Additionally, courtyard size and aspect ratio vary across different villages, influencing airflow and living comfort. This unique combination of traditional architecture and environmental adaptation underscores the significance of studying these courtyards to enhance sustainability in modern contexts.

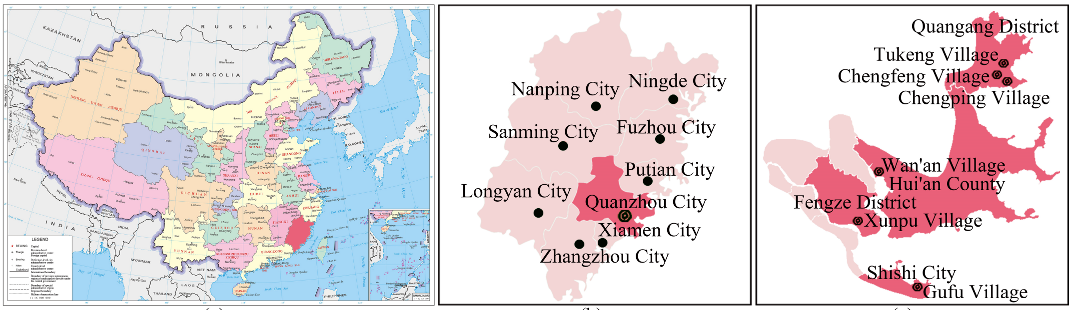

(a) (b) (c)

**Figure 1.** (**a**) China map. (**b**) Quanzhou map. (**c**) Location map of Quanzhou traditional village by the sea.

For this study, six coastal, traditional villages within Quanzhou Bay were selected (Figure 1c). Field measurements were carried out in the semi-public traditional residential courtyard spaces, including Minnan ancient residences and Fanzi buildings, which are relatively well preserved. This effort yielded a total of 204 sets of three-dimensional measurement data for typical traditional courtyard spaces.

Given these distinct architectural and climatic characteristics, this research aims to systematically explore how the spatial layout of courtyards affects the wind environment. The findings will contribute to both theoretical understanding and practical improvements in rural architectural design under changing environmental conditions.

#### 2.1.2. Enclosure Index of Spatial Layout Factors in Traditional Village Courtyards

This study was initiated to address the dual challenges posed by environmental changes and modernization in coastal villages. Quanzhou's traditional courtyards not only reflect historical architectural practices but also offer insights into environmental adaptation in the context of rising sea levels and increasing wind intensity. However, many of these spaces face threats from urbanization and the loss of traditional knowledge.

By focusing on the spatial layout indices of courtyards, this research aims to identify design strategies that enhance living comfort while preserving cultural heritage. The findings will also serve as a reference for future rural development projects in regions with similar climatic and environmental conditions.

The investigation of spatial layout factors influencing coastal courtyard forms in the Quanzhou Bay area focused on data collection for primary courtyard spatial layout indices. These indices were selected based on three criteria: (i) a significant correlation with the wind environment, (ii) the simplicity of model construction suitable for PHOENICS quantitative calculations, and (iii) the feasibility of field data collection or calculation [17]. The indices that satisfied all three criteria include courtyard area size, courtyard orientation, courtyard height-to-width ratio, courtyard aspect ratio, courtyard permeability, and courtyard height enclosure rate (as detailed in Table 1).

**Table 1.** Selection table of traditional village courtyard space layout indices.

| Courtyard Features | Layout Indices of the Courtyard Space | Wind Environment | Easy to Quantify with Phoenics | Easy to Conduct On-Site Research |
|---|---|---|---|---|
| Courtyard plan features | Planform | ✓ | | |
| | Courtyard area | ✓ | ✓ | ✓ |
| | Courtyard aspect ratio | ✓ | ✓ | ✓ |
| | Courtyard orientation | ✓ | ✓ | ✓ |
| Architectural features of the courtyard | Building height | ✓ | ✓ | |
| | Enclosure | ✓ | ✓ | |

**Table 1.** *Cont.*

| Courtyard Features | Layout Indices of the Courtyard Space | Wind Environment | Easy to Quantify with Phoenics | Easy to Conduct On-Site Research |
|---|---|---|---|---|
| Courtyard facade features | Permeability | ✓ | ✓ | |
| | Courtyard height-to-width ratio | ✓ | ✓ | |
| | Courtyard height deficit ratio | ✓ | ✓ | |
| Topographic and geomorphological features | Courtyard greening | ✓ | | |
| | Garden water body | ✓ | | |
| | Garden terrain | ✓ | | |

(1) Courtyard Spatial Layout Area Index

The courtyard area index pertains to the outdoor space linked with residential buildings, specifically the area enclosed by the buildings or walls that encompass it. This index is computed by multiplying the width and depth of the courtyard (Equation (1), Figure 2a), which quantifies the size of the courtyard space in this study.

$$S = L \times W \quad (1)$$

where S is the area of the courtyard space, L is the width of the courtyard, and W is the depth of the courtyard. The value of S is directly proportional to L and W; the larger the values of L and W, the larger the courtyard area. The courtyard area significantly impacts the wind environment: smaller areas result in reduced wind flow, while larger areas enhance wind flow. The size of the courtyard not only affects air circulation but also influences visual perception.

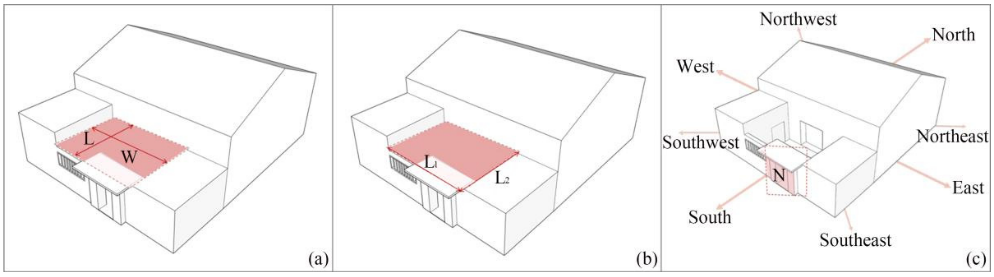


**Figure 2.** Indices of the courtyard plan's spatial layout: (**a**) area index; (**b**) aspect ratio index; (**c**) orientation index.

(2) Courtyard Spatial Layout Aspect Ratio Index

The aspect ratio index of a courtyard is defined as the ratio of the longer side to the shorter side of the courtyard's bounding rectangle (Equation (2), Figure 2b). This index quantifies the aspect ratio of the 204 courtyard spaces studied.

$$S = \frac{L_1}{L_2} \quad (2)$$

where S is the aspect ratio of the courtyard space, $L_1$ is the length of the courtyard's bounding rectangle, and $L_2$ is the width of the courtyard's bounding rectangle. If the aspect ratio is greater than 2, the courtyard is too narrow, which can affect ventilation or increase wind force. Courtyards with an aspect ratio of less than 2 are more square and have good centripetality, providing a more uniform visual distance during rest and tours, thus offering a stable and comfortable spatial experience [17].

(3) Courtyard Spatial Layout Orientation Index

The orientation of the courtyard refers to the direction of the courtyard's entrance (Equation (3), Figure 2c) rather than the orientation of the main building. The orientation information is primarily obtained through field measurements and is used to quantify the orientation of the 204 courtyard spaces studied.

$$S = N \tag{3}$$

where S is the numerical value of the courtyard's entrance orientation, and N represents the courtyard orientation in one of the eight cardinal directions. The orientation of the courtyard opening facilitates ventilation, heat dissipation, or thermal insulation, directly influencing courtyard comfort.

On this basis, data were organized for 204 traditional village courtyard spaces in AutoCAD v.2016 software (Figure 3). The width, depth, height, orientation, and total internal area of each courtyard space were statistically analyzed, and the area, orientation, and aspect ratio equations were, respectively, substituted to obtain the statistical table of the layout area, orientation, and aspect ratio values for the 204 traditional village courtyard spaces (Table 2).

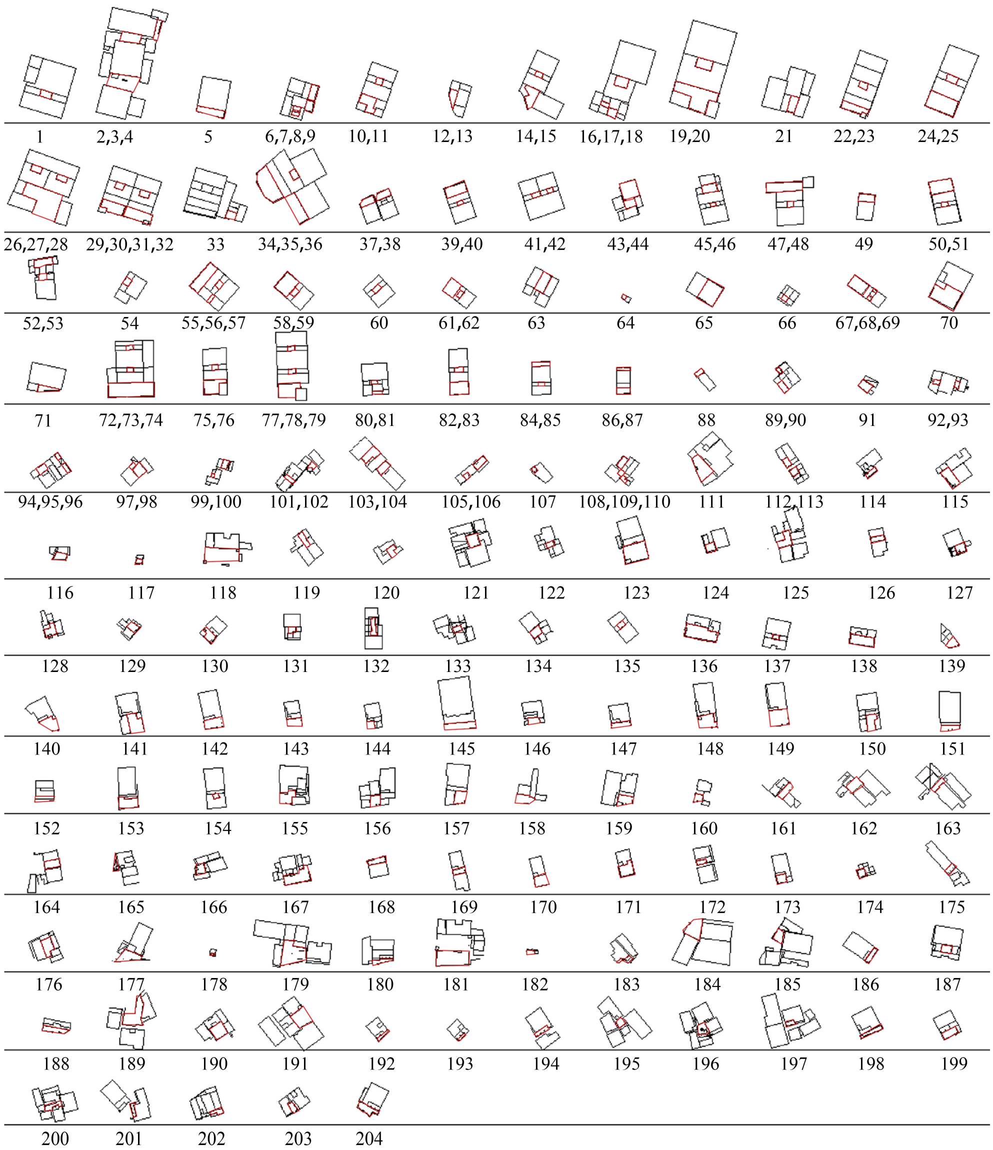


**Figure 3.** Layout plan of 204 courtyard spaces in traditional villages.

**Table 2.** Statistical table of the area, aspect ratio, and orientation index of 204 courtyard spatial layouts in traditional villages.

| No. | Area | L/W | Towards | No. | Area | L/W | Towards | No. | Area | L/W | Towards | No. | Area | L/W | Towards |
|---|---|---|---|---|---|---|---|---|---|---|---|---|---|---|---|
| 1 | 32.42 | 0.41 | SW | 52 | 50.85 | 0.47 | SE | 103 | 61.29 | 0.16 | NE | 154 | 29.00 | 0.36 | W |
| 2 | 146.78 | 0.81 | SE | 53 | 119.19 | 0.54 | SW | 104 | 42.44 | 0.54 | NW | 155 | 34.69 | 0.89 | SE |
| 3 | 80.07 | 1.17 | E | 54 | 18.26 | 0.79 | NW | 105 | 33.88 | 0.05 | NW | 156 | 39.26 | 0.66 | SE |
| 4 | 31.20 | 2.62 | E | 55 | 19.26 | 0.38 | SW | 106 | 12.18 | 1.00 | NW | 157 | 29.86 | 1.35 | SE |
| 5 | 72.17 | 0.98 | SW | 56 | 18.68 | 0.77 | NW | 107 | 9.15 | 0.73 | NW | 158 | 42.49 | 0.63 | SE |
| 6 | 12.42 | 0.75 | SW | 67 | 132.73 | 0.33 | SW | 108 | 28.96 | 0.53 | NW | 159 | 18.20 | 0.88 | S |
| 7 | 14.19 | 0.75 | SW | 58 | 18.06 | 0.82 | NW | 109 | 119.09 | 0.40 | SW | 160 | 27.02 | 0.35 | S |
| 8 | 30.57 | 0.12 | SE | 59 | 15.22 | 0.40 | NW | 110 | 12.54 | 0.93 | SE | 161 | 16.19 | 0.56 | SW |
| 9 | 42.78 | 0.08 | SE | 60 | 129.57 | 0.78 | SW | 111 | 13.70 | 0.61 | SW | 162 | 42.12 | 0.80 | SW |
| 10 | 84.98 | 0.44 | SW | 61 | 19.80 | 0.78 | NW | 112 | 21.48 | 0.65 | SW | 163 | 16.47 | 0.74 | SE |
| 11 | 20.29 | 0.71 | SW | 62 | 20.10 | 0.64 | NW | 113 | 20.46 | 0.84 | SW | 164 | 165.42 | 0.40 | S |
| 12 | 39.60 | 0.34 | W | 63 | 86.60 | 0.85 | SW | 114 | 17.45 | 0.36 | SE | 165 | 13.22 | 0.70 | SW |
| 13 | 61.32 | 0.44 | SW | 64 | 13.48 | 0.50 | NW | 115 | 77.18 | 0.10 | SW | 166 | 92.76 | 0.38 | SW |
| 14 | 13.78 | 0.64 | SW | 65 | 74.84 | 0.50 | NE | 116 | 85.98 | 0.46 | SW | 167 | 45.59 | 0.38 | SE |
| 15 | 33.90 | 0.44 | SW | 66 | 7.37 | 1.00 | NW | 117 | 34.69 | 0.69 | S | 168 | 61.90 | 0.64 | SE |
| 16 | 16.18 | 0.73 | SW | 67 | 17.08 | 0.85 | SE | 118 | 8.95 | 0.56 | S | 169 | 32.83 | 0.36 | SE |
| 17 | 54.46 | 0.61 | SW | 68 | 12.91 | 0.89 | SW | 119 | 4.38 | 0.33 | S | 170 | 10.90 | 0.43 | W |
| 18 | 288.77 | 0.09 | SW | 69 | 91.66 | 0.69 | SW | 120 | 162.43 | 0.76 | S | 171 | 33.60 | 1.03 | W |
| 19 | 65.88 | 0.59 | SW | 70 | 4.66 | 0.65 | NW | 121 | 29.16 | 0.17 | S | 172 | 94.80 | 0.53 | SE |
| 20 | 56.59 | 0.71 | SW | 71 | 6.12 | 0.89 | NW | 122 | 185.92 | 0.44 | S | 173 | 15.03 | 0.81 | SE |
| 21 | 24.92 | 1.08 | SW | 72 | 12.27 | 0.63 | SE | 123 | 231.12 | 0.50 | S | 174 | 36.92 | 0.59 | N |
| 22 | 78.35 | 0.13 | SW | 73 | 12.98 | 0.67 | SE | 124 | 12.20 | 0.51 | N | 175 | 26.66 | 0.58 | E |
| 23 | 31.98 | 0.50 | SW | 74 | 269.20 | 0.31 | SE | 125 | 40.15 | 0.77 | SE | 176 | 55.16 | 0.76 | E |
| 24 | 197.92 | 0.11 | SW | 75 | 101.59 | 0.61 | SE | 126 | 100.84 | 0.79 | SE | 177 | 61.28 | 0.76 | SE |
| 25 | 29.02 | 0.68 | SW | 76 | 14.36 | 0.74 | SE | 127 | 179.11 | 0.85 | SE | 178 | 19.46 | 0.50 | SE |
| 26 | 29.02 | 0.68 | SW | 77 | 128.62 | 0.60 | SE | 128 | 70.14 | 0.51 | SE | 179 | 33.06 | 0.80 | SE |
| 27 | 437.01 | 0.16 | SW | 78 | 13.45 | 0.66 | SE | 129 | 46.34 | 0.48 | S | 180 | 23.47 | 0.99 | SE |
| 28 | 105.41 | 0.12 | SW | 79 | 14.72 | 0.65 | SE | 130 | 21.57 | 0.98 | S | 181 | 11.17 | 0.54 | SW |
| 29 | 24.18 | 0.80 | SW | 80 | 12.01 | 0.28 | SE | 131 | 82.90 | 0.20 | SE | 182 | 71.29 | 0.58 | NW |
| 30 | 27.04 | 0.71 | SW | 81 | 8.82 | 0.74 | SE | 132 | 33.92 | 0.40 | SE | 183 | 110.21 | 0.76 | NW |
| 31 | 115.53 | 0.10 | SW | 82 | 102.23 | 0.69 | SE | 133 | 37.69 | 0.25 | SE | 184 | 57.59 | 0.96 | W |
| 32 | 35.77 | 0.51 | SW | 83 | 18.15 | 0.51 | SE | 134 | 103.89 | 0.80 | SE | 185 | 51.59 | 0.81 | SW |
| 33 | 87.25 | 0.10 | SW | 84 | 10.47 | 0.54 | NW | 135 | 129.54 | 0.87 | SE | 186 | 23.88 | 0.62 | SE |
| 34 | 32.54 | 0.61 | SW | 85 | 32.22 | 0.23 | NW | 136 | 76.97 | 0.50 | SE | 187 | 33.50 | 0.75 | SW |
| 35 | 174.34 | 0.06 | W | 86 | 14.17 | 0.18 | W | 137 | 35.90 | 0.25 | SE | 188 | 71.91 | 0.53 | SW |
| 36 | 27.59 | 0.73 | SW | 87 | 34.79 | 0.45 | SE | 138 | 36.60 | 0.13 | SE | 189 | 118.86 | 0.96 | N |
| 37 | 142.70 | 0.15 | SW | 88 | 18.74 | 0.52 | NW | 139 | 44.14 | 0.92 | S | 190 | 24.46 | 1.39 | SE |
| 38 | 229.22 | 0.78 | NW | 89 | 9.30 | 0.71 | NW | 140 | 41.81 | 0.86 | S | 191 | 60.78 | 0.60 | NW |
| 39 | 32.31 | 0.11 | S | 90 | 27.22 | 0.08 | SW | 141 | 61.00 | 1.13 | S | 192 | 141.40 | 0.79 | SE |
| 40 | 48.32 | 0.45 | NW | 91 | 45.11 | 0.16 | SW | 142 | 52.86 | 0.40 | W | 193 | 13.31 | 0.57 | SE |
| 41 | 42.13 | 0.48 | SW | 92 | 12.39 | 0.79 | W | 143 | 58.26 | 0.58 | S | 194 | 7.41 | 0.64 | SE |
| 42 | 9.77 | 0.58 | NW | 93 | 10.16 | 0.55 | NW | 144 | 23.17 | 0.91 | S | 195 | 29.25 | 0.78 | NE |
| 43 | 89.93 | 0.46 | NW | 94 | 14.92 | 0.35 | NE | 145 | 46.13 | 0.56 | S | 196 | 22.97 | 0.92 | NW |
| 44 | 13.15 | 0.84 | SE | 95 | 29.12 | 0.68 | NW | 146 | 34.00 | 0.30 | NW | 197 | 49.68 | 0.79 | NW |
| 45 | 26.02 | 0.72 | SE | 96 | 9.71 | 0.06 | NW | 147 | 29.34 | 0.70 | SE | 198 | 15.44 | 0.55 | W |
| 46 | 120.12 | 0.99 | SW | 97 | 52.07 | 0.12 | SE | 148 | 62.38 | 0.92 | SE | 199 | 26.04 | 0.55 | W |
| 47 | 42.79 | 0.73 | NW | 98 | 21.10 | 0.72 | NE | 149 | 17.36 | 0.68 | SE | 200 | 48.05 | 0.45 | SE |
| 48 | 9.97 | 0.84 | SW | 99 | 16.12 | 0.36 | NW | 150 | 124.26 | 0.56 | SE | 201 | 17.99 | 0.62 | S |
| 49 | 53.74 | 0.56 | NW | 100 | 12.88 | 0.77 | E | 151 | 60.08 | 0.32 | SE | 202 | 40.91 | 0.65 | SE |
| 50 | 136.45 | 0.24 | SW | 101 | 26.47 | 0.77 | S | 152 | 34.02 | 0.83 | SW | 203 | 49.38 | 0.52 | SE |
| 51 | 15.26 | 0.88 | W | 102 | 4.76 | 0.87 | W | 153 | 20.59 | 0.90 | SE | 204 | 20.34 | 0.52 | SE |

### *2.2. Contrastive Research Method*

In this study, PHOENICS 2016 was chosen as the primary software for CFD simulations due to its specialization in fluid dynamics and heat transfer applications. PHOENICS has been extensively used in architectural and environmental research, providing reliable simulations for complex airflow patterns. Its RNG k-ε turbulence model is particularly suitable for capturing high-strain rate flows common in courtyard spaces.

This study examines the courtyard spaces of 204 coastal, traditional villages in Quanzhou City. From these, representative original models were abstracted to create 18 comparative models based on three key indices: area, orientation, and aspect ratio. These models facilitate a comparative analysis of the winter wind environment, illustrating how variations in courtyard layout affect comfort during winter.

For the comparative analysis, SketchUp 2021 software was utilized to construct models of the 18 traditional village courtyard indices. In these models, architectural details such as roofs and dougong (traditional bracket sets) were excluded to focus on the relationship between courtyard spatial layout indices and winter wind environment comfort. These idealized models were then imported into Phoenics software to conduct Computational Fluid Dynamics (CFD) simulations.

*2.3. Research Ideas*

The study adopts a comprehensive approach, combining mathematical analysis, field measurements, simulations, and comparative research to evaluate the impact of courtyard spatial layouts on the wind environment. The research follows a systematic process:

1. Problem Identification: Based on gaps in existing research, this study focuses on the effects of courtyard size, aspect ratio, and orientation on wind comfort in traditional rural villages in Quanzhou.
2. Data Collection and Model Construction: A total of 204 courtyard spaces were selected as research subjects, and representative models were constructed to highlight key spatial indices.
3. Simulation and Analysis: Computational Fluid Dynamics (CFD) simulations were performed to model the wind environment within these courtyard spaces.
4. Validation through Field Measurements: Measurements were conducted to validate simulation results and identify discrepancies, with a focus on optimizing courtyard design for winter conditions.
5. Result Interpretation and Application: The findings provide actionable insights into how traditional courtyard layouts can be adapted to modern needs while maintaining environmental sustainability.

The core research idea is to bridge traditional architectural knowledge with modern computational tools to develop design strategies that enhance environmental comfort and resilience. The research framework and its components are depicted in Figure 4.

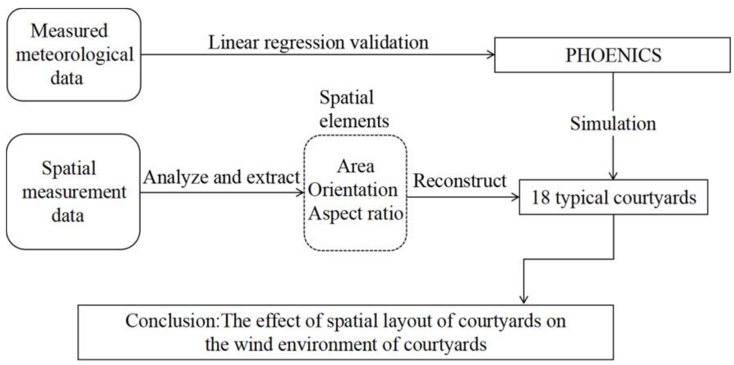


**Figure 4.** Research ideas.

*2.4. Evaluation Methods and CFD Simulation*

2.4.1. Evaluation Criteria for Winter Wind Environment

This study evaluates the impact of courtyard layout factors on the winter wind environment within traditional villages. The evaluation criteria are derived from the "Chinese Green Building Evaluation Standard" and prior research. According to the "Evaluation Standard for Green Building" (GB/T 50378-2019), optimal conditions are defined as maintaining a ground wind pressure difference between the windward and leeward sides of a building of no less than 0.5 Pa and no more than 5 Pa under typical winter wind conditions to prevent cold air infiltration [18]. Building on research by Chen, L.; Du, Y.; and Ghasemi, Z. et al., wind speed zones are categorized into a still wind zone (0 to 0.5 m/s), a comfortable wind zone (0.5 to 2.0 m/s), and a strong wind zone (over 2.0 m/s) [19–21]. To evaluate wind conditions, wind speed data at a height of 1.5 m above ground level is utilized, as recommended by both the aforementioned standard and empirical research.

2.4.2. Details of the Wind Environment Experiment and Simulations

(1) Measured Points Selection

To effectively analyze the typical horizontal flow fields within traditional village courtyard spaces and pinpoint the optimal locations for winter wind environment measurements, Computational Fluid Dynamics (CFD) was employed to simulate the wind environment for a specific courtyard case (Courtyard No. 109). This simulation aids in understanding the behavior of natural winter winds as they interact with the courtyard. Measurement points were strategically selected based on their positions within different flow field regions shaped by these interactions. The points are designated as follows: A (due north), B (northwest), C (due west), D (southwest), E (due south), F (southeast), G (due east), H (northeast), and I (center). These points correspond to specific areas of airflow dynamics, including the windward area, corner flow area, through flow area, vortex area, and wind shadow area, as depicted in Figure 5a.

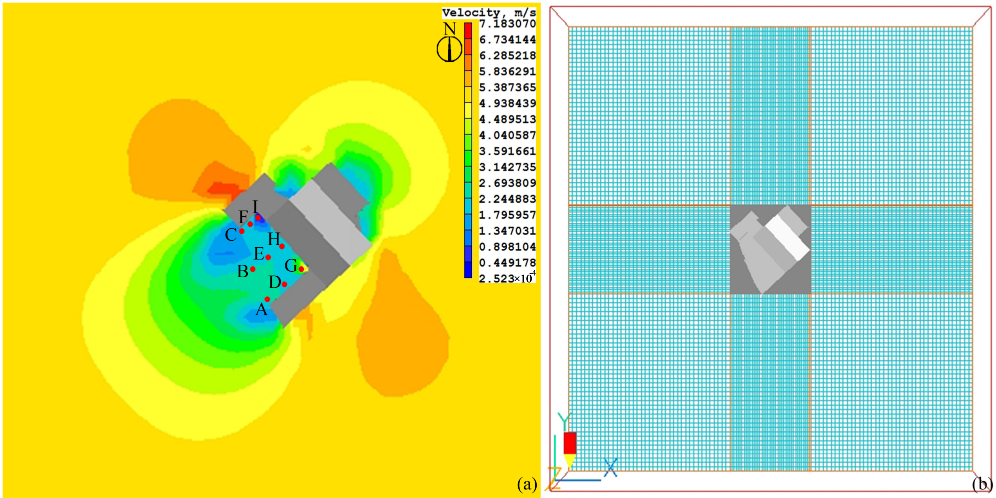


**Figure 5.** (**a**) Distribution map of wind speed measurement points. (**b**) PHOENICS mesh settings.

(2) Field Experiment Method

To ensure the validity of the coupling between measured and simulated wind speed values, this study capitalized on the pronounced variability of wind forces in the coastal villages of Quanzhou Bay, characterized by elevated wind speeds during strong wind events. The chosen date for the field measurements was 10 January 2024, from 9:00 a.m. to 5:00 p.m., selected for its clear and mostly cloudless conditions. Measurements were taken using the Kestrel 5500 handheld weather meter. Employing a fixed-point observation method with multiple observers, measurements were conducted at nine designated points (A, B, C, D, E, F, G, H, I) within Courtyard No. 109 in the Xunpu community. The setup for wind environment simulation scenarios subsequently mirrored these measurement points.

Each measurement station involved a wind speed meter mounted on a tripod, with the anemometer inlet positioned 1.5 m above the ground. Data were recorded hourly, with each data point representing the average wind speed over a 1 min interval. Minimum, average, and maximum wind speeds were recorded every 10 s. This protocol yielded 9 sets comprising 486 effective wind speed data points from 9:00 a.m. to 5:00 p.m. The average wind speed data for each hour was statistically analyzed and compared to assess the actual wind conditions at different points in the courtyard. The accuracy of the wind speed measurements using the NK500LNK weather meter is ±3%.

(3) Three-Dimensional Model Construction

The values of the most frequently occurring indices for the three key layout factors of traditional village courtyard spaces—area, orientation, and aspect ratio—were statistically derived from Table 1. These indices helped to summarize the typical original model for the wind comfort simulation experiments of traditional village courtyard spaces, ensuring general applicability.

In terms of courtyard area, the index most frequently falls within the 20 to 80 square meter range, accounting for 50.73% of observations. Regarding orientation, the southeast direction is the most common, making up 31.7% of the data. For the aspect ratio, the range of 0.5 to 0.7 is the most frequent, representing 35.61% of the cases. Based on these findings, a typical original model of a traditional village courtyard space was established (Figure 6). The model parameters were set with a courtyard area of 50 $m^2$, an orientation facing southeast, and an aspect ratio of 0.6. These configurations aim to facilitate comparative analysis of wind comfort differences influenced by variations in these three indices. The courtyard spaces in 204 traditional villages were analyzed based on their area, aspect ratio, and orientation. They were classified into five area index types: 20, 50, 110, 170, and 230 square meters (Figure 7a–e). The aspect ratio classifications included indices of 0.32, 0.60, 0.80, 1.00, and 1.20 (Figure 7f–j). The orientation index classifications comprised southeast, southwest, west, northeast, south, east, northwest, and north (Figure 7k–r). Eighteen index models were developed from typical original models, corresponding to the specified areas, aspect ratios, and orientation indices. The simplified integer values of the 18 index models are detailed in Table 3.

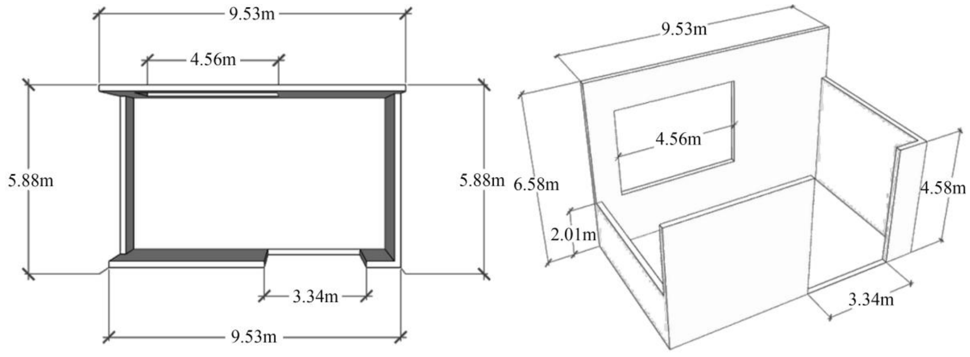


**Figure 6.** (**a**) Original model plan. (**b**) Three-dimensional model.

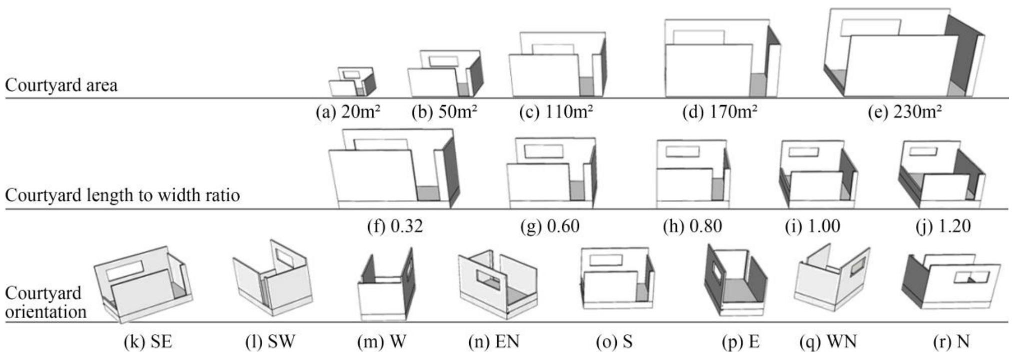


**Figure 7.** Three-dimensional models with different indices.

**Table 3.** Simplified values for exponential models in traditional village courtyards.

| No. | Numerical Value | No. | Numerical Value | No. | Numerical Value |
|---|---|---|---|---|---|
| a | 5.40 × 3.40 × 3.50 | b | 9.53 × 5.96 × 5.56 | c | 13.94 × 8.52 × 5.77 |
| d | 17.23 × 10.55 × 9.42 | e | 20.60 × 20.60 × 5.40 | f | 17.20 × 17.20 × 5.40 |
| g | 5.93 × 5.88 × 6.58 | h | 20.60 × 20.60 × 6.40 | i | 20.60 × 20.60 × 5.40 |
| j | 23.10 × 23.10 × 5.40 | k | 9.53 × 5.96 × 5.56 | l | 9.53 × 5.96 × 5.56 |
| m | 9.53 × 5.96 × 5.56 | n | 9.53 × 5.96 × 5.56 | o | 9.53 × 5.96 × 5.56 |
| p | 9.53 × 5.96 × 5.56 | q | 9.53 × 5.96 × 5.56 | r | 9.53 × 5.96 × 5.56 |

(4) CFD Simulation Settings

For Computational Fluid Dynamics (CFD) simulations, a variety of software options are available, such as PHOENICS, ANSYS FLUENT, ENVI-met, Airpak, and Butterfly. Among these, PHOENICS stands out as the world's first commercial software developed specifically for CFD and heat transfer applications. It is widely used in the simulation of wind environments in residential areas, school districts, and landscape gardens. The use of PHOENICS in previous studies has demonstrated its effectiveness in various contexts: different height distribution patterns have been shown to influence changes in wind speed and pressure [22], modifications in building layouts can significantly reduce community energy consumption and carbon emissions [23], and the arrangement of courtyard plants can greatly affect outdoor microclimates and enhance residents' comfort regarding wind and thermal conditions [24]. Additionally, alterations in building spatial layout and aspect ratios have been effective in creating ecological buffer zones [25]. Therefore, PHOENICS is deemed suitable for simulating the wind environment in the courtyard spaces of this study.

The specific CFD simulation settings and model setup in PHOENICS are as follows:

Model Selection: The RNG k-ε turbulence model is chosen for its robustness in handling high strain rates and complex flows, as specified in PHOENICS. This model is implemented as shown in Equations (4) and (5).

Discretization Scheme: The PRESTO! scheme is used for discretizing the pressure field, ensuring enhanced accuracy in scenarios with sharp gradients and complex geometries.

Velocity–Pressure Coupling: The built-in PARSOL (Partial Cell) function facilitates the execution of velocity–pressure coupling simulations, particularly beneficial in environments with complex boundaries and obstructions, using a fine-scale mesh to enhance calculation accuracy.

Convergence Detection: PHOENICS's automatic convergence detection system ensures that simulation results achieve reasonable convergence, with a targeted convergence accuracy of $10^{-5}$ [26]. This system helps verify that the simulation outcomes are stable and reliable across different simulation scenarios.

These settings are meticulously designed to simulate the nuanced wind dynamics within traditional village courtyards, aiming to produce data that can effectively inform design decisions and environmental adjustments to enhance comfort and sustainability in coastal village settings.

$$\frac{\partial(\rho k)}{\partial t} + \frac{\partial(\rho k u_i)}{\partial x_i} = \frac{\partial}{x_j}\left(\alpha_k \eta_{eff} \frac{\partial k}{\partial x_j}\right) + G_k + \rho\varepsilon \tag{4}$$

$$\frac{\partial(\rho \varepsilon)}{\partial t} + \frac{\partial(\rho \varepsilon v_i)}{\partial x_i} = \frac{\partial}{\partial x_j}\left(\alpha_\varepsilon \eta_{\Delta f} \frac{\partial \varepsilon}{\partial x_j}\right) + \frac{C^*_{1s}\varepsilon}{k} G_k - C_{2s}\rho \frac{\varepsilon^2}{k} \tag{5}$$

In the equations, turbulent kinetic energy is denoted by $k$, and the turbulent dissipation rate is denoted by $\varepsilon$.

Mesh Settings: The computational domain for the CFD simulations is set to dimensions significantly larger than those of the actual scene model to ensure that boundary effects do not influence the results. Specifically, the length and width of the computational domain are established at five times the length and width of the scene model, respectively, and the height is set to three times that of the scene model. The mesh within this domain is categorized into two regions: central and edge. In the central region, where higher resolution is critical for capturing detailed flow patterns, the planar mesh density is set to 4 m × 4 m, with a vertical mesh density of 0.5 m. Conversely, the edge region, which typically experiences less variation in airflow, features a coarser planar mesh density of 8 m × 8 m and a vertical mesh density of 1 m. This strategic mesh configuration optimizes the balance between simulation accuracy and computational efficiency, reducing the number of mesh segments and thereby enhancing the time efficiency of the simulations (Figure 5b).

Wind Condition Settings: For wind conditions, this study adheres to the "Code for Design of Heating, Ventilation, and Air Conditioning in Civil Buildings" [27]. Additionally, wind data from sources such as the "China Weather Network", "China Meteorological Network", and "China Meteorological Data Network" indicate that the average winter wind speed in the Quanzhou area is 6.13 m/s, predominantly from the northeast. These specifics are incorporated into the inflow boundary condition of the simulations. The simulations are iterated 2000 times to ensure the stability and accuracy of the results. The ground roughness coefficient, denoted as $\alpha$, is set to 0.2, reflecting the typical ground surface roughness of the region, which affects wind flow behavior near the ground. This setting is crucial for accurately simulating wind interactions with the complex geometries of traditional village courtyards and their surroundings.

## 3. Results

### *3.1. Comparative Analysis of Measured and Simulated Values*

Based on CFD simulations of the wind environment in Courtyard No. 109 in the Xunpu community, an average wind speed of 6.3 m/s was used as the inflow wind speed in the CFD simulations. During the CFD simulation experiments, the positions of the measurement points from the field measurements (points A, B, C, D, E, F, G, H, I) were placed into the wind field simulation environment. The average wind speeds at these points were recorded, and the simulated wind field data at each measurement point were compared with the field measurement data (Figure 8).

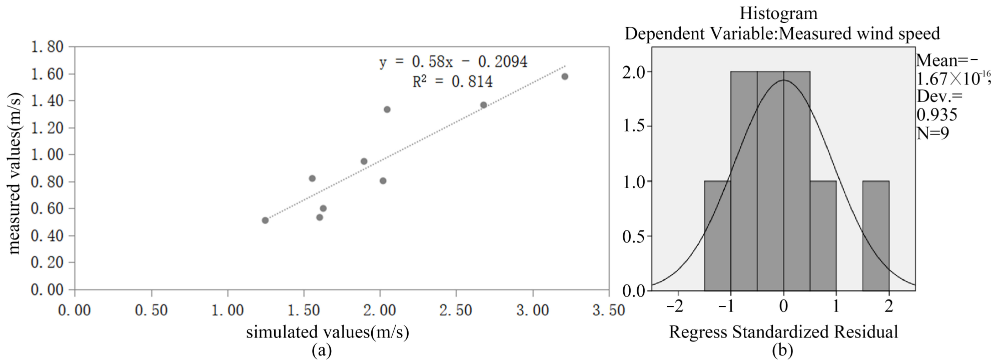


**Figure 8.** (**a**) Linear regression plot of measured and CFD simulated values. (**b**) Histogram of regression normalised residuals.

As shown in Table 4 and Figure 8a, the $R^2$ value is 0.814, indicating that 81.4% of the variation in the measured wind speeds can be explained by the simulated wind speeds. The high linear regression value between the simulated and measured wind speeds indicates that the PHOENICS software provides a strong linear fit and is highly feasible. The regression equation is Y = 0.58X − 0.2094. From Table 5, a $p$-value less than 0.5 indicates significant linear regression characteristics. Additionally, the residuals follow a normal distribution (Figure 8b), suggesting a well-constructed model. This demonstrates that PHOENICS is effective in simulating the wind environment in courtyard spaces.

**Table 4.** Model summary [b].

| Model | R | R Squared | Adjusted R Squared | Std. Error of the Estimate | Durbin–Watson |
|---|---|---|---|---|---|
| 1 | 0.903 [a] | 0.814 | 0.790 | 0.181 | 1.424 |

[a] Predictors (constant): simulated wind speed. [b] Dependent variable: measured wind speed.

**Table 5.** ANOVA [a].

| Model | | Sum of Squares | df | Mean Squared | F | Sig. |
|---|---|---|---|---|---|---|
| 1 | Regression | 1.019 | 1 | 1.019 | 31.017 | 0.001 [b] |
| | Residual | 0.230 | 7 | 0.033 | | |
| | Total | 1.249 | 8 | | | |

[a] Dependent variable: measured wind speed. [b] Predictors (constant): simulated wind speed.

### 3.2. Impact of Courtyard Spatial Layout Factors on Wind Environment

To assess the influence of various courtyard spatial layout factors—specifically courtyard area size, orientation, and aspect ratio—on the wind environment, PHOENICS software was utilized to conduct CFD simulations across 18 traditional village courtyard space index models. Measurements of wind speed and wind pressure were taken at a pedestrian height of 1.5 m above the ground (Z = 1.5 m), providing a detailed analysis of these variables.

#### 3.2.1. Effect of Yard Area Index on Wind Environment

Wind Speed (Figure 9a–e): Table 6 reveals that the winter wind speeds across five different courtyard areas ranged from 0.716 to 3.355 m/s. Notably, the fourth courtyard showed the greatest variation in wind speed, with a minimum of 2 m/s and a maximum of 3.62 m/s, resulting in a wind difference of 1.62 m/s. The fifth, third, and first courtyards followed in terms of variation, while the second courtyard exhibited the smallest variation, with a wind difference of only 0.981 m/s. Across the 45 wind speed measurement points in the five courtyards, 42.22% were categorized within the comfortable wind speed range (0.5–2 m/s), none within the uncomfortable range (less than 0.5 m/s), and 57.77% in the strong wind range (greater than 2 m/s). The fourth courtyard had the most points with uncomfortable wind speeds, followed by the third and fifth courtyards, while the second and first courtyards reported no uncomfortable wind speed points. The analysis indicates that larger courtyard areas in winter are more susceptible to strong wind conditions, which can affect wind comfort.

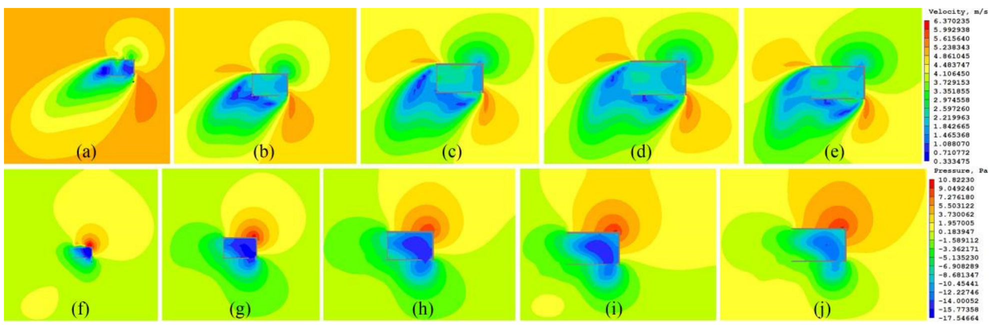


**Figure 9.** Winter wind speed and pressure maps of the courtyard area index: (**a**–**e**) wind speed; (**f**–**j**) wind pressure.

Wind Adjustment Range: According to Table 7, under constant conditions with variations only in courtyard area, the wind adjustment ranges in winter for courtyard areas of 15 $m^2$, 50 $m^2$, 110 $m^2$, 170 $m^2$, and 230 $m^2$ were 74.14%, 74.57%, 78.60%, 77.65%, and 69.30%, respectively. The courtyard of 110 $m^2$ displayed the most favorable wind adjustment range, being 1.06 times that of the 15 $m^2$ courtyard. The courtyard area of 230 $m^2$ had the lowest wind adjustment range among all the courtyard sizes.

**Table 6.** Statistics table of the courtyard area index for winter wind speed.

| No. | Area (m²) | Wind Speed at Monitoring Point m/s | | | | | | | | | Wind Difference |
|---|---|---|---|---|---|---|---|---|---|---|---|
| | | A | B | C | D | E | F | G | H | I | |
| 1 | 15 | 0.860 | 1.305 | 1.224 | 0.969 | 0.716 | 1.133 | 1.582 | 1.199 | 1.767 | 1.051 |
| 2 | 50 | 1.523 | 1.604 | 1.815 | 1.019 | 1.060 | 2.000 | 1.986 | 2.000 | 1.615 | 0.981 |
| 3 | 110 | 2.270 | 2.855 | 1.713 | 2.347 | 2.611 | 2.297 | 2.009 | 2.994 | 2.810 | 1.281 |
| 4 | 170 | 2.615 | 3.139 | 2.202 | 2.586 | 3.355 | 3.620 | 2.000 | 2.960 | 2.737 | 1.620 |
| 5 | 230 | 3.282 | 2.105 | 1.902 | 2.737 | 2.812 | 2.881 | 2.383 | 2.652 | 1.979 | 1.380 |

Note: Red is the highest wind speed and wind difference for each of the 5 courtyard spaces, green is the lowest wind speed and wind difference for each of the 5 courtyard spaces, blue is the detection point where the wind speed is less than 0.5 m/s for each of the 5 courtyard spaces (the lowest wind speed detection point is no longer marked in green in this case), and the mid-grey underlining is for the courtyard spaces with uncomfortable wind speed detection points.

**Table 7.** Statistical table of winter wind adjustment range for courtyard area index.

| No. | Courtyard Area | Input Wind Speed | Average Wind Speed | Wind Adjustment Range | Wind Adjustment Ratio |
|---|---|---|---|---|---|
| 1 | 15 $m^2$ | 6.13 | 1.585 | 74.14% | 1.00 |
| 2 | 50 $m^2$ | 6.13 | 1.559 | 74.57% | 1.01 |
| 3 | 110 $m^2$ | 6.13 | 1.312 | 78.60% | 1.06 |
| 4 | 170 $m^2$ | 6.13 | 1.370 | 77.65% | 1.05 |
| 5 | 230 $m^2$ | 6.13 | 1.882 | 69.30% | 0.93 |

Note: Wind amplitude = 1 − average wind speed/input wind speed; a positive number indicates that the wind amplitude is reduced; a negative number indicates that the wind amplitude is raised contrary to the reduced wind amplitude; the wind multiplier = the wind amplitude n/wind amplitude 1—labeled red for the different areas of the index of five kinds of courtyard space wind multiplier highest, and labeled green for the different areas of the index of five kinds of courtyard space wind multiplier lowest.

Wind Pressure (Figure 9f–j): Table 8 indicates that the maximum wind pressure differences in winter for the five different courtyard areas ranged from 2.518 to 10.933 Pa in Quanzhou Bay's coastal, traditional villages. The highest recorded wind pressure difference was 10.933 Pa, and the lowest was 2.518 Pa. Notably, 80% of the courtyards experienced wind pressure differences exceeding 5 Pa, which could potentially lead to conditions that could adversely affect physical and mental health. Only the first courtyard had a wind pressure difference below 5 Pa, suggesting higher wind comfort. The statistical analysis further reveals that as the courtyard area increased, so did the overall wind pressure difference, with the third courtyard experiencing the highest pressure difference and the first experiencing the lowest.

**Table 8.** Statistics table of the courtyard area index for winter wind pressure.

| No. | Area ($m^2$) | Maximum Air Pressure Difference | No. | Area ($m^2$) | Maximum Air Pressure Difference |
|---|---|---|---|---|---|
| 1 | 15 $m^2$ | 2.518 | 4 | 170 $m^2$ | 9.551 |
| 2 | 50 $m^2$ | 6.737 | 5 | 230 $m^2$ | 9.474 |
| 3 | 110 $m^2$ | 10.933 | - | - | - |

Note: The red label is the largest of the five different sizes of courtyard spaces with their respective maximum wind pressure difference values, the green label is the smallest of the five different sizes of courtyard spaces with their respective maximum wind pressure difference values.

### 3.2.2. Impact of Aspect Ratio Index on Wind Environment

Wind Speed (Figure 10a–e): Table 9 reveals that the winter wind speeds in five different aspect ratio courtyard spaces in Quanzhou Bay's coastal, traditional villages range from 0.526 to 2.453 m/s. The first courtyard shows the most significant variation in wind speed, with a minimum of 0.526 m/s and a maximum of 2.428 m/s, resulting in a wind difference of 1.902 m/s. It is followed by the fourth, third, and second courtyards, with the fifth courtyard displaying the smallest variation at a wind difference of only 0.757 m/s.

Remarkably, all 45 wind speed measurement points across the five courtyards fall within the comfortable wind speed range (0.5–2 m/s), with no instances of uncomfortable or strong winds. The distribution of uncomfortable wind speed detection points, from most to least, is found in the first, fifth, and third courtyards. Statistical analysis of these points suggests that as the aspect ratio increases, the occurrence of uncomfortable wind detection points fluctuates, with courtyards having ratios of 0.8 and 1.2 experiencing no uncomfortable wind detection points.

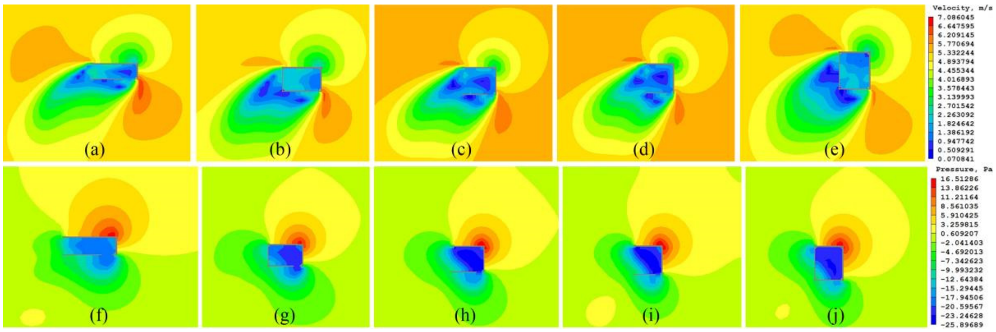


**Figure 10.** Winter wind speed and pressure maps of the courtyard aspect ratio index: (**a**–**e**) wind speed; (**f**–**j**) wind pressure.

**Table 9.** Statistics table of the courtyard aspect ratio index for winter wind speed.

| No. | H/W | Wind Speed at Monitoring Point m/s | | | | | | | | | Wind Difference |
|---|---|---|---|---|---|---|---|---|---|---|---|
| | | A | B | C | D | E | F | G | H | I | |
| 1 | 0.32 | 1.114 | 1.663 | 2.428 | 1.211 | 1.020 | 0.526 | 1.926 | 2.332 | 1.454 | 1.902 |
| 2 | 0.6 | 1.393 | 1.983 | 2.135 | 1.315 | 1.760 | 2.178 | 1.489 | 2.293 | 1.983 | 0.978 |
| 3 | 0.8 | 1.040 | 1.586 | 1.771 | 1.284 | 0.985 | 1.335 | 1.693 | 1.970 | 1.693 | 0.985 |
| 4 | 1 | 1.200 | 1.757 | 1.868 | 1.772 | 1.330 | 2.004 | 2.453 | 1.617 | 1.564 | 1.253 |
| 5 | 1.2 | 1.236 | 1.436 | 1.651 | 1.646 | 0.894 | 1.291 | 1.339 | 1.105 | 1.435 | 0.757 |

Note: Red is the highest wind speed and wind difference for each of the 5-yard spaces, green is the lowest wind speed and wind difference for each of the 5-yard spaces, blue is the detection point where the wind speed is less than 0.5 m/s for each of the 5-yard spaces (the lowest wind speed detection point is no longer marked in green in this case), and the mid-gray underlining is for the yard spaces containing uncomfortable wind speed detection points.

Wind Adjustment Range: According to Table 10, under conditions where only the courtyard aspect ratio changes, the wind adjustment ranges in winter for courtyards with ratios of 0.32, 0.6, 0.8, 1, and 1.2 are 75.22%, 70.03%, 75.79%, 71.79%, and 78.19%, respectively. The courtyard with an aspect ratio of 1.2 exhibits the highest wind adjustment range, 1.04 times that of the courtyard with a ratio of 0.32, while the courtyard with a ratio of 0.6 displays the lowest wind adjustment range.

**Table 10.** Statistical table of winter wind adjustment range for courtyard aspect ratio index.

| No. | H/W | Input Wind Speed | Average Wind Speed | Wind Adjustment Range | Wind Adjustment Ratio |
|---|---|---|---|---|---|
| 1 | 0.32 | 6.13 | 1.519 | 75.22% | 1.00 |
| 2 | 0.6 | 6.13 | 1.837 | 70.03% | 0.93 |
| 3 | 0.8 | 6.13 | 1.484 | 75.79% | 1.01 |
| 4 | 1 | 6.13 | 1.729 | 71.79% | 0.95 |
| 5 | 1.2 | 6.13 | 1.337 | 78.19% | 1.04 |

Note: Wind amplitude = 1 − average wind speed/input wind speed, a positive number indicates that the wind amplitude is reduced, a negative number indicates that the wind amplitude is raised contrary to the wind amplitude is reduced, the wind multiplier = the wind amplitude n/wind amplitude 1; the red labeled for the different aspect ratio of the five kinds of courtyard space wind multiplier is the highest, and the green labeled for the different aspect ratio of the five kinds of courtyard space wind multiplier is the lowest.

Wind Pressure (Figure 10f–j): Table 11 indicates that the maximum wind pressure differences in winter for the five different aspect ratio courtyard spaces range from 0.193 to 5.806 Pa. The highest recorded wind pressure difference is 5.806 Pa and the lowest is 0.193 Pa. Only 20% of the courtyards have a wind pressure difference exceeding 5 Pa, signaling the presence of strong winds that could potentially affect physical and mental health. Notably, only the third courtyard has a wind pressure difference below 0.5 Pa, indicative of still wind conditions and poor air circulation within the courtyard. As the aspect ratio increases, the overall wind pressure difference in the courtyard spaces decreases. The first courtyard registers the largest pressure difference, while the third courtyard shows the smallest. Statistical analysis of the uncomfortable wind pressure detection points across the five ideal models indicates that larger aspect ratios correspond to fewer uncomfortable wind detection points.

**Table 11.** Statistics table of the courtyard aspect ratio index for winter wind pressure.

| No. | H/W | Maximum Air Pressure Difference | No. | H/W | Maximum Air Pressure Difference |
|---|---|---|---|---|---|
| 1 | 0.32 | 5.806 | 4 | 1 | 1.216 |
| 2 | 0.6 | 2.517 | 5 | 1.2 | 1.089 |
| 3 | 0.8 | 0.193 | - | - | - |

Note: The red label is the largest of the five different aspect ratios of the respective maximum wind pressure difference values in the courtyard space, the green label is the smallest of the five different aspect ratios of the respective maximum wind pressure difference values in the courtyard space, and the medium gray background is the courtyard space containing a wind pressure difference of less than 0.5 Pa and higher than 5 Pa.

### 3.2.3. Impact of Courtyard Orientation Index on Wind Environment

Wind Speed (Figure 11a–h): According to Table 12, the winter wind speeds across eight differently oriented courtyard spaces range from 0.013 to 3.951 m/s. The sixth courtyard, which is oriented east, shows the greatest variation in wind speed, with a minimum of 0.71 m/s and a maximum of 3.951 m/s, resulting in a wind difference of 3.241 m/s. This is followed by the third, eighth, and second courtyards. Conversely, the fourth courtyard, showing the least variation, has a wind difference of only 0.585 m/s. Out of a total of 72 wind speed measurement points, 90.28% fall within the comfortable wind speed range (0.5–2 m/s), 6.94% are within the uncomfortable range (less than 0.5 m/s), and 2.78% are within the strong wind range (greater than 2 m/s). Courtyards oriented northwest and west have the most uncomfortable wind speed points, followed by those oriented southeast and north. Courtyards facing southwest, south, and northeast exhibit the highest wind comfort. Statistical analysis indicates that different orientations affect the occurrence of uncomfortable wind detection points during winter, with courtyards oriented northeast experiencing no uncomfortable wind detection points.

Wind Adjustment Range: As shown in Table 13, with constant conditions and only changes in courtyard orientation, the wind adjustment ranges in winter for courtyards oriented east, southeast, south, southwest, west, northwest, north, and northeast are 80.10%, 77.29%, 67.75%, 72.50%, 67.29%, 65.45%, 86.13%, and 75.97%, respectively. The courtyard oriented towards the northwest has the best wind adjustment range, which is 1.08 times that of the courtyard facing the southeast, while the courtyard oriented towards the east has the lowest wind adjustment range.

Wind Pressure (Figure 11i–p): Table 14 reveals that the maximum wind pressure differences in winter for the eight differently oriented courtyard spaces range from 1.708 to 8.819 Pa. The highest wind pressure difference is 8.819 Pa and the lowest is 1.708 Pa. Some 37.5% of the courtyards experience wind pressure differences greater than 5 Pa, indicating the presence of strong winds that could adversely affect physical and mental health. The third, sixth, and seventh courtyards, with wind pressure differences above 5 Pa, are categorized as strong wind areas. Among these, the sixth courtyard (oriented east) has the highest pressure difference, while the fifth courtyard (oriented south) records the lowest. Statistical analysis shows that courtyards with higher wind pressure differences, particularly those oriented west, east, and northwest, generally result in poorer human comfort during winter.

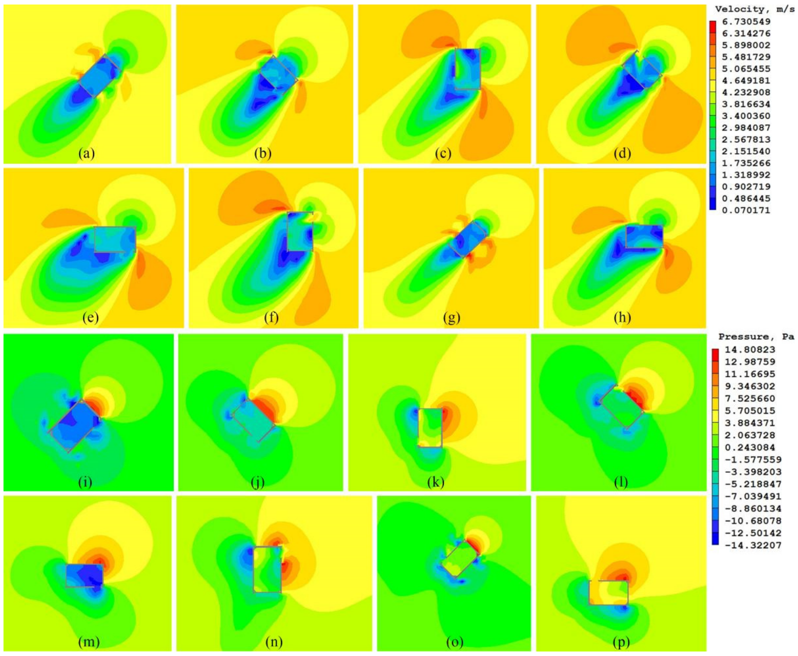


**Figure 11.** Winter wind speed and pressure maps of the courtyard orientation index: (**a**–**h**) wind speed; (**i**–**p**) wind pressure.

**Table 12.** Statistics table of the courtyard orientation index for winter wind speed.

| No. | Courtyard Orientation | Wind Speed at Monitoring Point m/s A | B | C | D | E | F | G | H | I | Wind Difference |
|---|---|---|---|---|---|---|---|---|---|---|---|
| 1 | SE | 1.129 | 1.621 | 0.885 | 1.445 | 1.913 | 0.439 | 0.961 | 1.577 | 1.007 | 1.474 |
| 2 | SW | 0.921 | 1.038 | 1.713 | 0.693 | 1.553 | 1.541 | 1.290 | 1.547 | 2.229 | 1.533 |
| 3 | W | 2.381 | 3.314 | 2.293 | 1.906 | 2.199 | 0.330 | 1.990 | 1.407 | 1.971 | 2.984 |
| 4 | NE | 1.969 | 1.429 | 1.924 | 1.506 | 1.619 | 1.574 | 1.976 | 1.786 | 1.391 | 0.585 |
| 5 | S | 1.885 | 2.235 | 2.038 | 1.429 | 2.053 | 2.273 | 2.567 | 1.593 | 1.974 | 1.138 |
| 6 | E | 2.165 | 2.731 | 1.117 | 2.408 | 2.458 | 1.058 | 2.462 | 0.710 | 3.951 | 3.241 |
| 7 | NW | 1.219 | 0.947 | 0.013 | 1.223 | 0.990 | 1.369 | 0.623 | 1.046 | 0.219 | 1.356 |
| 8 | N | 2.206 | 2.521 | 1.297 | 0.451 | 1.476 | 1.050 | 1.638 | 1.617 | 1.005 | 2.07 |

Note: Red is the highest wind speed and wind difference for each of the 8-yard spaces, green is the lowest wind speed and wind difference for each of the 8-yard spaces, blue is the detection point where the wind speed is less than 0.5 m/s for each of the 8-yard spaces (the lowest wind speed detection point is no longer marked in green in this case), and the mid-gray underlining is for the yard spaces containing uncomfortable wind speed detection points.

**Table 13.** Statistical table of winter wind adjustment range for courtyard orientation index.

| No. | Courtyard Orientation | Input Wind Speed | Average Wind Speed | Wind Adjustment Range | Wind Adjustment Ratio |
|---|---|---|---|---|---|
| 1 | SE | 6.13 | 1.220 | 80.10% | 1.00 |
| 2 | SW | 6.13 | 1.392 | 77.29% | 0.96 |
| 3 | W | 6.13 | 1.977 | 67.75% | 0.85 |
| 4 | NE | 6.13 | 1.686 | 72.50% | 0.91 |
| 5 | S | 6.13 | 2.005 | 67.29% | 0.84 |
| 6 | E | 6.13 | 2.118 | 65.45% | 0.82 |
| 7 | NW | 6.13 | 0.850 | 86.13% | 1.08 |
| 8 | N | 6.13 | 1.473 | 75.97% | 0.95 |

Note: Wind amplitude = 1 − average wind speed/input wind speed, a positive number indicates that the wind amplitude is lowered, a negative number indicates that the wind amplitude is raised contrary to the wind amplitude, wind multiplier = wind amplitude n/wind amplitude 1; red is the highest wind multiplier for 8 kinds of courtyard spaces with different orientations, and green is the lowest wind multiplier for 8 kinds of courtyard spaces with different orientations.

**Table 14.** Statistics table of the courtyard orientation index for winter wind pressure.

| No. | Courtyard Orientation | Maximum Air Pressure Difference | No. | Courtyard Orientation | Maximum Air Pressure Difference |
|---|---|---|---|---|---|
| 1 | SE | 2.776 | 5 | S | 1.708 |
| 2 | SW | 4.013 | 6 | E | 8.819 |
| 3 | W | 5.968 | 7 | NW | 5.698 |
| 4 | NE | 3.807 | 8 | N | 4.726 |

Note: Marked red is the largest of the 8 patio spaces with their respective maximum wind pressure difference values, marked green is the smallest of the 8 patio spaces with their respective maximum wind pressure difference values, and the mid-gray background is the patio space containing a wind pressure difference of less than 0.5 Pa and more than 5 Pa.

## 4. Discussion

### *4.1. Impact of Courtyard Layout Factors on Wind Environment*

The findings of this study highlight the significant influence of courtyard spatial layouts on the wind environment of coastal, traditional village courtyards during winter. Specifically, the results emphasize that the interplay between courtyard area, aspect ratio, and orientation can effectively enhance wind comfort, contributing to both livability and cultural heritage preservation. By systematically examining these factors, this study provides a more comprehensive understanding of the adaptive measures employed in traditional architecture to mitigate adverse environmental conditions.

The analysis of different courtyard areas reveals that courtyards with medium areas (e.g., 50 $m^2$) demonstrate optimal winter wind comfort due to their ability to balance airflow without generating excessive wind shadows or stagnant air pockets. This finding underscores the value of medium-sized courtyards in traditional architectural practices, aligning with the principles of maximizing comfort while maintaining spatial efficiency (Figure 12a). In contrast, larger courtyards tend to create distinct windward and leeward zones, which can reduce comfort levels by causing significant temperature drops and cold air accumulation.

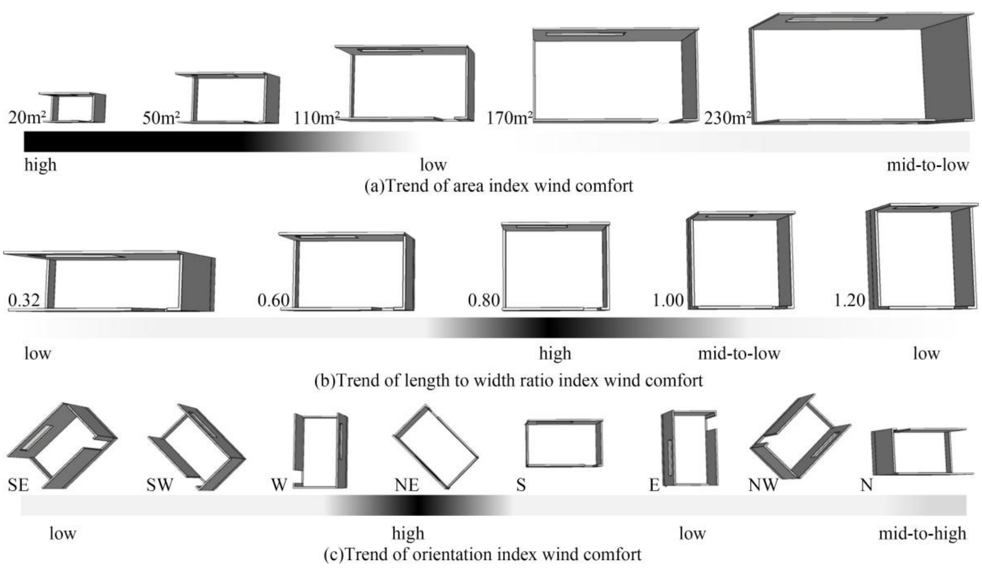


**Figure 12.** Trend chart of wind comfort based on three indices: area, aspect ratio, and orientation.

Aspect ratio also plays a critical role in influencing wind comfort, with ratios between 0.8 and 1.2 being found to provide the most stable and comfortable airflow distribution. This result suggests that a balance between width and height is key to maintaining comfortable wind conditions within courtyard spaces. Aspect ratios greater than 1.2 were found to create narrow, high-speed wind paths, which can negatively affect comfort (Figure 12b).

The orientation of courtyards emerged as another crucial factor. The results indicate that northeast, southeast, and northwest orientations are particularly effective for mitigating the effects of winter winds, as these orientations facilitate airflow while preventing direct wind exposure. This finding is supported by the measured wind comfort levels across different orientations, as illustrated in Figure 12c. Such orientations align with the dominant wind patterns in coastal areas, demonstrating the practical wisdom of traditional courtyard design in adapting to local climatic conditions.

The combined analysis of area, aspect ratio, and orientation reveals that the optimal design for a winter courtyard in traditional coastal villages includes a medium area, an aspect ratio between 0.8 and 1.2, and a northeast orientation. This integrated approach allows for improved airflow, minimizes wind shadow effects, and maximizes overall comfort. These findings provide valuable insights for both preserving traditional architecture and designing new, climate-adapted rural spaces. Moreover, the study highlights the need for a holistic approach that considers multiple spatial layout indices to enhance wind comfort, echoing previous recommendations in architectural environmental research.

### 4.2. Comparison with Previous Studies

This study aligns with findings from research in other regions. Similar to studies in Inner Mongolia, the results show that small, enclosed courtyards create more comfortable microclimates. Research from Wuhan and northeastern China emphasizes that wind comfort is significantly influenced by orientation and architectural layout, a finding echoed by this study's focus on optimizing southeast and northeast orientations. However, differences were observed: in northeastern China, courtyards oriented towards the south performed better during winter, while in Quanzhou, southeast-facing courtyards were more effective due to the region's unique coastal wind patterns.

### 4.3. Research Limitations

While this study has produced significant insights, there are some limitations. The CFD simulations were conducted using idealized courtyard models, which may not fully capture the complexity of real-world courtyard environments. Factors such as roof forms, vegetation, and architectural details were not included in the models, which could influence the wind environment in significant ways. Future research should incorporate these elements to obtain a more comprehensive understanding of wind comfort in traditional courtyards. Additionally, expanding the study to other seasons would provide a year-round assessment of courtyard comfort, thus offering a more complete evaluation of these spaces' environmental adaptability.

## 5. Conclusions

This study systematically examines the impact of courtyard layout on the winter wind environment in traditional coastal villages in Quanzhou, focusing on the effects of courtyard area, aspect ratio, and orientation. The findings reveal that a moderate courtyard area (e.g., 50 $m^2$), an aspect ratio between 0.8 and 1.2, and an orientation towards the northeast or southeast provide optimal winter wind comfort by balancing wind flow distribution and mitigating strong wind impacts. These insights not only validate the traditional architectural wisdom inherent in courtyard designs but also provide a scientific basis for improving living comfort in traditional rural environments.

The research highlights the importance of considering the combined effects of different courtyard layout factors in designing traditional village courtyards. By integrating appropriate areas, aspect ratios, and orientations, architects can enhance the wind environment, providing a comfortable living space while preserving the cultural heritage of traditional settlements. This holistic approach to courtyard design addresses both the aesthetic and environmental needs of rural communities, making it especially relevant in the context of ongoing environmental and social changes.

Despite its contributions, the study has certain limitations. The use of idealized models in Computational Fluid Dynamics (CFD) simulations does not capture the full complexity of architectural details such as roofs, openings, and vegetation, which may influence the wind environment. Future research should incorporate these elements to gain a more comprehensive understanding of the wind dynamics within traditional village courtyards. Additionally, expanding the study to include different seasons will provide a more complete evaluation of the year-round wind comfort in these spaces.

Overall, this study provides valuable insights into designing courtyard layouts to optimize winter wind comfort. It offers practical recommendations that can be applied to rural development projects. By combining traditional architectural practices with modern computational tools, this research contributes to sustainable rural development and the preservation of cultural heritage in coastal regions.

**Author Contributions:** Conceptualization, Z.W. and S.D.; methodology, Y.W., J.C. and S.D.; software, T.H., Y.Z. and S.D.; validation, Z.W., S.D., J.C. and Y.W.; formal analysis, Z.W., S.D., Y.Z. and Y.W.; investigation, Z.W., J.C. and Y.W.; resources, Z.W.; data curation, Z.W., J.C. and T.H.; writing—original draft preparation, Z.W., J.C., F.T. and S.D.; writing—review and editing, Z.W., S.D., Y.W. and F.T.; visualization, T.H., F.T. and Y.Z.; supervision, S.D., T.H. and Y.W.; project administration, Z.W.; funding acquisition, Z.W. All authors have read and agreed to the published version of the manuscript.

**Funding:** This study received funding from the National Natural Science Foundation of China Youth Science Fund Project [42401236], the General Project for Fujian Province Natural Science Foundation in China [2023J01894], the Ministry of Education through the Humanities and Social Science Research Youth Fund projects [21YJCZH006], and the Fujian Young and Middle-Aged Teacher Education Research projects [JAT210303].

**Data Availability Statement:** The original contributions presented in the study are included in the article. Further inquiries can be directed to the corresponding authors.

**Conflicts of Interest:** No conflicts of interest have been declared by the authors.

## References

1. Hayakawa, K.; Miyaoka, D. CFD (Computational Fluid Dynamics) on the Wind Environment of the Gassho-Style Houses in Shirakawa-mura Ogimachi. *Urban Hous. Sci.* **2012**, *14*, 14–19.
2. Ai, Z.; Mak, C. CFD Simulation of Flow in a Long Street Canyon Under a Perpendicular Wind Direction: Evaluation of Three Computational Settings. *Build. Environ.* **2017**, *114*, 293–306. [CrossRef]
3. Villagrán, E.; Flores-Velazquez, J.; Akrami, M.; Bojacá, C. Influence of the Height in a Colombian Multi-Tunnel Greenhouse on Natural Ventilation and Thermal Behavior: Modeling Approach. *Sustainability* **2021**, *13*, 13631. [CrossRef]
4. Emmanuel, M.R. *An Urban Approach to Climate-Sensitive Design*; Spon Press: London, UK, 2005.
5. Zhao, Y.; Chen, Y.; Li, K. A Simulation Study on the Effects of Tree Height Variations on the Façade Temperature of Enclosed Courtyard in North China. *Build. Environ.* **2021**, *207*, 108566. [CrossRef]
6. Chang, C.; Meroney, N.R. Concentration and Flow Distributions in Urban Street Canyons: Wind Tunnel and Computational Data. *J. Wind Eng. Ind. Aerodyn.* **2003**, *91*, 1141–1154. [CrossRef]
7. Li, Z.; Wu, S.; Zhao, Q. Field Measurement and Evaluation of the Outdoor Wind Environment in Dimen Dong Village, Guizhou. *J. Archit. Therm. Vent. Air Cond.* **2015**, *34*, 27–30.
8. Ying, X.; Han, X.; Huangfu, F.; Liang, X.; Qin, X.; Gao, Q. Layout of Exhibition Buildings under the Dual Objectives of Courtyard Size and Wind Environment. *J. Harbin Inst. Technol.* **2022**, *54*, 1–10.
9. Dang, Y. Study on the Impact of Enclosed Teaching Building Forms on Courtyard Wind Environment in Wuhan Universities. Master's Thesis, Huazhong University of Science and Technology, Wuhan, China, 2022. [CrossRef]
10. Chen, K. Research on the Characteristics and Optimization of Courtyard Wind Environment in Rural Residences in Central and Western Inner Mongolia. Master's Thesis, Inner Mongolia University of Technology, Hohhot, China, 2022. [CrossRef]
11. Zhang, L.; Hou, J.; Yu, Y.; Du, J.; Meng, X.; He, Q. Numerical Simulation of Outdoor Wind Environment of Typical Traditional Village in the Northeastern Sichuan Basin. *Procedia Eng.* **2017**, *205*, 923–929. [CrossRef]
12. Yang, L.; Liu, X.; Qian, F.; Niu, S. Research on the Wind Environment and Air Quality of Parallel Courtyards in a University Campus. *Sustain. Cities Soc.* **2020**, *56*, 102019. [CrossRef]

13. Sözen, I.; Oral, G.K. Outdoor Thermal Comfort in Urban Canyon and Courtyard in Hot Arid Climate: A Parametric Study Based on the Vernacular Settlement of Mardin. *Sustain. Cities Soc.* **2019**, *48*, 101398. [CrossRef]
14. Sharples, S.; Bensalem, R. Airflow in Courtyard and Atrium Buildings in the Urban Environment: A Wind Tunnel Study. *Sol. Energy* **2001**, *70*, 237–244. [CrossRef]
15. Wang, J. Research on Strategies to Improve the Wind Environment of Village Residential Courtyards in Severe Cold Regions of Northeast China. Master's Thesis, Harbin Institute of Technology, Harbin, China, 2016.
16. Wang, Y.; Lu, T.; Jiang, S.; Zhu, H. Field Measurement and Simulation Analysis of Wind Environment at Village Entrance Spaces in Traditional Villages of Eastern Jiangxi: A Case Study of Jinxi County. *J. Guilin Univ. Technol.* **2021**, *41*, 111–122.
17. Shao, W.; Li, Z.; Ye, M. Study on the Courtyard Spatial Form and Elements of Huizhou Traditional Residences Based on Cluster Analysis. *South Archit.* **2022**, *1*, 76–84.
18. *GB/T 50378-2019*; Evaluation Standard for Green Building. China Architecture & Building Press: Beijing, China, 2019; pp. 126–127.
19. Chen, L.; Mak, C.M. Integrated Impacts of Building Height and Upstream Building on Pedestrian Comfort Around Ideal Lift-Up Buildings in a Weak Wind Environment. *Build. Environ.* **2021**, *200*, 107963. [CrossRef]
20. Du, Y.; Mak, C.M.; Liu, J.; Xia, Q.; Niu, J.; Kwok, K. Effects of Lift-Up Design on Pedestrian Level Wind Comfort in Different Building Configurations Under Three Wind Directions. *Build. Environ.* **2017**, *117*, 84–99. [CrossRef]
21. Ghasemi, Z.; Esfahani, M.A.; Bisadi, M. Promotion of Urban Environment by Consideration of Human Thermal & Wind Comfort: A Literature Review. *Procedia-Soc. Behav. Sci.* **2015**, *201*, 397–408. [CrossRef]
22. Lu, M.; Song, D.; Shi, D.; Liu, J.; Wang, L. Effect of High-Rise Residential Building Layout on the Spatial Vertical Wind Environment in Harbin, China. *Buildings* **2022**, *12*, 705. [CrossRef]
23. Xuan, W. Research on Reducing Carbon Consumption in Residential Community Spaces as Influenced by Microclimate Environments. *J. Urban Plan. Dev.* **2021**, *9*, 147.
24. Li, J.; Liu, J.; Srebric, J.; Hu, Y.; Liu, M.; Su, L.; Wang, S. The Effect of Tree-Planting Patterns on the Microclimate within a Courtyard. *Sustainability* **2019**, *11*, 1665. [CrossRef]
25. Xu, X.; Luo, F.; Wang, W.; Hong, T.; Fu, X. Performance-Based Evaluation of Courtyard Design in China's Cold-Winter Hot-Summer Climate Regions. *Sustainability* **2018**, *10*, 3950. [CrossRef]
26. Chu, C.-R.; Su, Z.-Y. Natural Ventilation Design for Underground Parking Garages. *Build. Environ.* **2022**, *227*, 109784. [CrossRef]
27. *GB50736-2012*; Code for Design of Heating, Ventilation and Air Conditioning in Civil Buildings. China Construction Industry Press: Beijing, China, 2012; pp. 47–50.